TOTAL ENERGY AND ENERGY DISTRIBUTION IN A LASER CRYSTAL DUE TO OPTICAL PUMPING, AS CALCULATED BY THE MONTE CARLO METHOD

By D. R. Skinner* and J. Tregellas-Williams*

[*Manuscript received July* 30, 1965]

Summary

The Monte Carlo technique is applied to discover the total absorbed energy and its distribution within a laser crystal in complex pumping systems not amenable to normal analysis. Allowance is made for: the effects of multiple reflections, both specular and diffuse; modification of Lambert-law emission by refraction at flash-lamp envelopes; the effect of laser crystal absorptivity on total absorbed energy; and the use of phosphors for increasing the efficiency of utilization of pump radiation by effectively broadening the crystal absorption bands. The results are in good agreement with previous experimental work and with less comprehensive theoretical treatments of simple systems. The effects of multiple reflections, both specular and diffuse, and of uneven energy distribution on overall laser efficiency are demonstrated quantitatively.

I. Introduction

The optical pumping of suitable crystals to induce laser action is frequently accomplished by the focusing action of elliptical cylinders, either single or in symmetrical "clover-leaf" clusters (Fig. 1). (See for example, Ciftan *et al.* 1961; Bowness, Missio, and Rogala 1962.)

The overall efficiency (η_T) of a solid-state laser, at a given pumping level, may be defined as the ratio of output to input energies and thus depends on the amount of pump-band energy absorbed in the laser crystal and on the way in which it is converted to coherent radiation. We may therefore write

$$\eta_T = \eta_L \cdot \eta_t \cdot \eta_c \,, \tag{1}$$

where

$$\eta_L = E_P/E_I \qquad \text{(lamp efficiency)}, \tag{2}$$

$$\eta_t = E_c/E_P \qquad \text{(transfer efficiency)}, \tag{3}$$

$$\eta_c = E_o/E_c \qquad \text{(conversion efficiency)}, \tag{4}$$

in which E_I is the electrical energy input to the lamp, E_P is the energy emitted by the lamp either in the laser pump-band or capable of conversion to the pump-band by the use of fluorescent materials other than the laser crystal, E_c is the part of E_P that is absorbed in the crystal, and E_o is the energy of the stimulated radiation output.

The threshold of a laser, although affected by η_t, also appears to be dependent on the energy density distribution within the crystal.

This paper is concerned primarily with presenting a method for estimating η_t and the energy distribution within a laser crystal for elliptical (and cylindrical) pumping systems. Individual rays are traced through the cavity from the flash-lamp,

* Defence Standards Laboratories, Department of Supply, Maribyrnong, Vic.

using three-dimensional coordinate geometry. In Figure 2(a), a ray is seen to undergo several refractions in the lamp envelope and water-jacket before being reflected at the cavity wall, first specularly and then as from a diffuse surface, the choices being made at random according to the respective probabilities of these and other possible operations on the ray. On arrival at the laser crystal the ray may undergo refraction, as shown, or reflection. Absorption into the crystal is studied by dividing its volume into many segments (Fig. 2(b)) and summing the energy deposited in each section over all rays considered. On leaving the crystal, the attenuated ray continues its track until further tracking would be unprofitable. The method requires few restrictive assumptions.

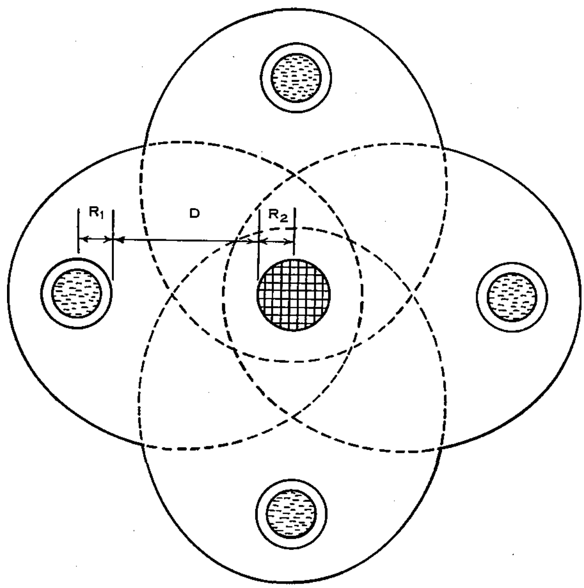

Fig. 1.—Arrangement of four flash-tubes and a laser crystal in a confocal clover-leaf cavity.

The transfer efficiency η_t has been calculated by several workers using different simplifying premises. Schuldt and Aagard (1963) considered one reflection only at the wall of a single elliptical cylinder and complete absorption within the crystal; they further based their calculations on infinitely long Lambertian sources and laser rods. The interactions of eccentricity, radius ratio of source to laser, and source radius to semimajor axis ratio with efficiency were treated and trends deduced. Calculations have been made for single and multiple elliptical cylinders by Fried and Eltgroth (1962), Ackerman (1963), and Bowness (1965) using similar assumptions, but, as the present paper shows, serious inaccuracies in forecasting efficiencies result from ignoring multiple reflections and the modification of Lambert's law by refraction at the flash-lamp envelope.

Computations of the energy distribution within a laser crystal have attracted more attention; the effects of radial pumping of the laser rod (Tomiyasu 1962) and of the sapphire-clad ruby (Devlin *et al.* 1962; McKenna 1963) have been calculated using two-dimensional models. The three-dimensional case has been analysed for radial and isotropic illumination of simple and composite laser crystals (McKenna 1963; Sooy and Stitch 1963; Cooke, McKenna, and Skinner 1964). Experimental verification of the non-uniform distribution of light within a laser rod has been made (Skinner 1964) for the two-dimensional case, and the irregularities in the output of a

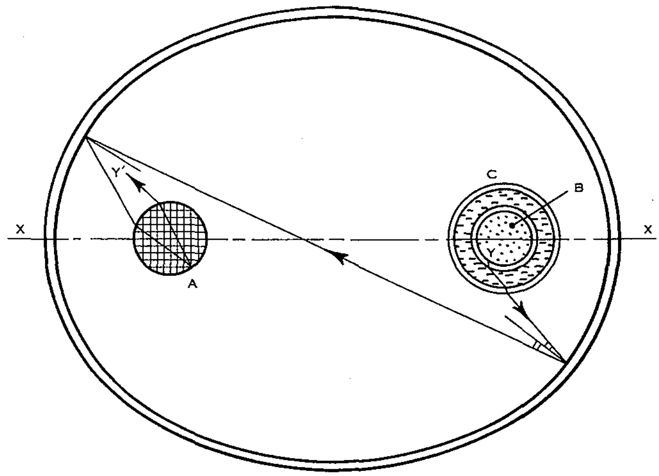

Fig. 2(*a*).—A single elliptical cavity showing the laser crystal (A), flash-lamp (B), water jacket (C), plane of symmetry (X–X), and the start of a ray track (Y–Y′).

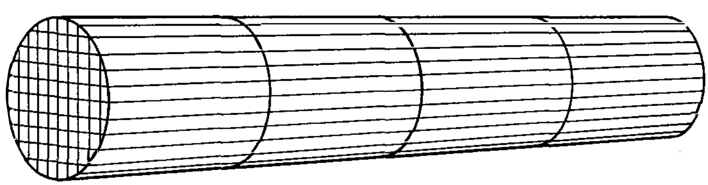

Fig. 2(*b*).—Typical reduction of a laser crystal to segments for analysis of energy density distribution.

ruby laser have been discussed qualitatively with reference to the pumping uniformity (Li and Sims 1962). No calculations of the energy distribution to be expected in a practical system have yet appeared.

In order to present a realistic model of the system and to allow for the use of fluorescent materials to effect an apparent broadening of the laser crystal absorption band, the model used here can take account simultaneously of the following departures from ideal behaviour.

(i) The pumping cavity may be either a single or a multiple elliptical cylinder (which includes the special case of a circular cylinder).

(ii) Allowance is made for multiple reflections within the cavity, including those from the plane ends.

(iii) Both the curved cavity walls and the plane ends may give rise to specular and diffuse reflection, fluorescence, and absorption in any proportions.

(iv) Cylindrical refracting surfaces and partially transparent, fluorescent components can be simulated.

(v) The treatment is three-dimensional.

(vi) Source-blocked rays may be re-emitted with a specified efficiency.

(vii) The transfer efficiency of the cavity and the energy density distribution within the laser crystal are computed simultaneously for the same system.

Since these specifications render an analytical solution impracticable, the system has been simulated on a high speed digital computer by using the Monte Carlo technique (Householder 1949); in essence, this involves studying the course of a random sample of events in a mathematical model of the system, rather than analysing the behaviour of the general event. In the problem under consideration, the random events correspond to rays of light leaving the flash-tube and a study is made of the histories of their progression through the cavity to ultimate absorption.

II. General Approach

(a) *Input and Output of the Computer*

The aim of the computer program can be readily seen by examining the input and output requirements. The main input data are:

(i) the types of components within the pumping cavity, e.g. laser crystals, flash-lamps, water jackets;

(ii) the positions and dimensions of the components;

(iii) the optical properties of the components; and

(iv) the number of ray tracks to be considered (usually 1000) and the maximum number of intersections (i.e. points at which rays meet component surfaces) in each track (usually 20).

The main output consists of:

(v) a statement of the energy deposited in various parts of the system;

(vi) a matrix giving energy density in the various segments within the laser crystal; and

(vii) a diagram showing contours of equal energy density at a number of cross sections of the laser crystal; these are obtained by finding the average energy density in a series of slices (usually four) taken along the axis of the crystal.

(b) *Organization of the Computing*

Because of its length and complexity, the calculation is split up in two ways. The contour plotting is separated from the main part of the calculation for convenience in computing; the main calculation is carried out by a controlling program (Fig. 3) that can call upon a series of subprograms, thus allowing similar blocks of instructions to be used at various points in the program without the need for rewriting.

The flow diagram shows that, in calculations for systems having features in common, it is not necessary to read in the full data for each system, since provision is made for re-entry to the data input at various points. This facility includes a re-entry with no new data, in which case the previous calculation is repeated with a new random selection of ray tracks.

The tracing of a track involves many cycles of a closed path, starting with the choice of the next intersection and passing through one of seven subprograms representing models for intersections with various types of components. These models

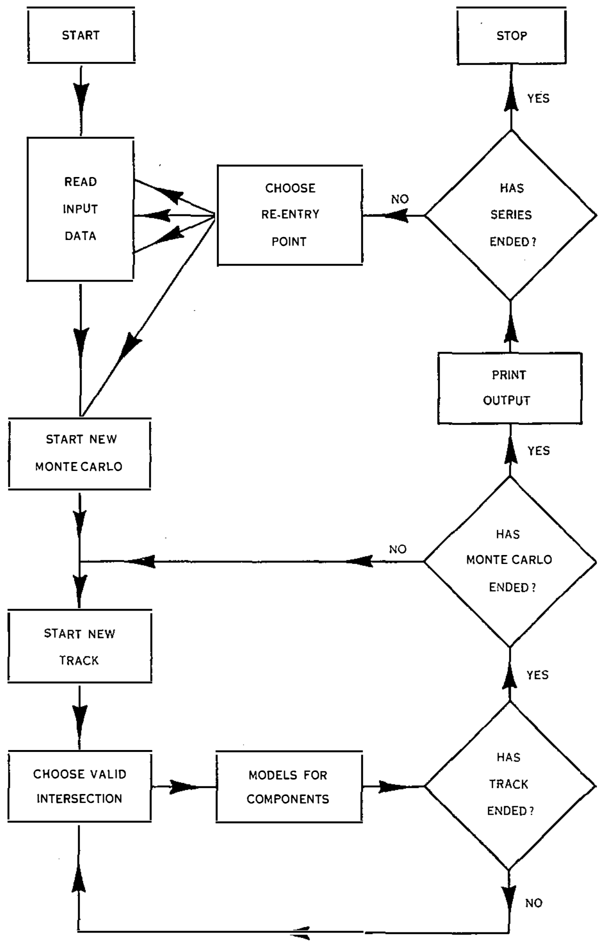

Fig. 3.—Flow diagram for the computer program.

give new values for the origin, direction, and intensity of the ray, and control is returned to the beginning of the cycle. The ray is abandoned when its intensity falls below an amount specified in the data (usually 1 % of the original intensity) or when the number of intersections with components exceeds the specified value (usually 20). In a perfectly reflecting cavity, the only loss mechanisms for the light are absorption in the laser crystal and escape via the ends of the flash-lamps. Much of the loss recorded as wasted absorption in this case is due to the termination of tracks after 20 intersections, and therefore the true efficiencies are higher than those computed. This error is significant only for highly reflecting surfaces and, even then, approximate extrapolation to an infinite number of intersections may be made from an analysis of wasted absorption into real and computational losses. A pseudo-random number generator (Rotenberg 1960) is used, suitably weighted, to choose the path of a ray at points where it divides, such as on diffuse reflection or at a refracting surface (see Appendix).

(c) *Smoothing and Contour Plotting*

One would expect certain symmetries, due to geometrical arrangements, to be present in the energy density matrix, but, because of the random nature of the calculation, corresponding densities are not equal. An improvement in accuracy, and therefore in smoothness, can be obtained by averaging such values.

Rotation and addition of the energy density matrices is necessary for systems containing more than one flash-lamp, since ray-traces are started from one lamp only. These operations are carried out by a program that produces, by linear interpolation, contours of constant energy density. Contours appear outside the outline of the laser crystal owing to interpolation to the zero values at the corner of the matrix but these do not affect the accuracy of the remaining contours.

III. Description of Mathematical Models

(a) *Pumping Cavity*

The cavity may be a single elliptical cylinder or a clover leaf with up to 10 lobes, not necessarily confocal. The length is finite and the perpendicular end walls are made of the same material as the curved sides. Data are fed into the program to specify the proportions of light that undergo specular and diffuse reflection, fluorescence, and absorption; these are assumed to be independent of the angle of incidence of the ray. Diffuse reflection and fluorescent emission are assumed to follow Lambert's law (Appendix) and separate data are used to specify the behaviour of fluorescent light thus produced.

(b) *Flash-lamp*

The flash-lamp is considered to be two concentric cylinders, the plasma and the envelope. The plasma is assumed to be a Lambert-law emitter and to re-emit any rays striking it. An alternative assumption would be that the incident ray is transmitted through the plasma, but the real situation is complex and between these extremes (Emmett, Schawlow, and Weinberg 1964). However, the work of Bowness (1965) implies that, even if the radiation striking the plasma were ignored completely, the error would be small so that the effect of assuming one particular form of re-emission would be very small indeed. The envelope is considered to be a refracting cylinder with no absorption. Rays reaching the envelope from the outside are reflected or refracted with probabilities given by the Fresnel equations (Appendix). From within, light is refracted out with reduced intensity due to internal reflection.

(c) *Laser Crystal*

The laser crystal is considered as a cylinder of absorbing material with an absorption coefficient* that may be modified at will to explore the effects of different doping concentrations on energy distribution. A further absorption coefficient may be prescribed for the cases where pump light has been converted to more favourable narrow-band radiation by a fluorescent coating or solution. In common with other models, the absorption coefficient is invariate with flux density. Dielectric reflective coatings on the ends of the laser crystal may be simulated by the assignment of a high refractive index to these surfaces. The crystal is divided into 100 or 400 rectangular segments in cross section and up to 5 in length. If a ray strikes the crystal, a choice between reflection and refraction is made as for the flash-lamp envelope. In the case of refraction, the path of the ray is computed and the amount of energy deposited in each segment is recorded. When the far surface of the crystal is reached, a further selection is made between internal reflection and refraction. Internal reflection results in a repetition of the energy deposition process.

When the incident ray is below a specified intensity, a penetration depth is calculated (Appendix) at which the whole of the remaining energy is deposited. If the depth exceeds the computed path length, the ray passes to its next intersection with no reduction in intensity.

(d) *Fluorescent Solids and Liquids*

Fluorescent solids and liquids other than the laser crystal may be simulated by absorbent refractive cylinders. Any light absorbed is assumed to produce isotropic fluorescence (Appendix) at the same point with a specified quantum efficiency. The absorption coefficient is different for pump and fluorescent light.

(e) *Other Components*

Provision is made for two other classes of component to be within the pumping cavity. These may be used to simulate such objects as sapphire cladding around a ruby or cooling systems and collets holding components. The first type is a non-absorbing refractive cylinder, and the second is an imperfectly reflecting cylinder producing absorption and specular reflection in specified proportions.

IV. Accuracy

In a series of experiments in each of which N shots are fired at a target with an expected score of n hits, the expected variance of the scores recorded is given by

$$\sigma^2 = Npq\,, \tag{5}$$

where σ^2 is the variance (σ the standard deviation), p the probability of a hit, and q the probability of a miss ($q = 1-p$). It follows that

$$\sigma^2 = n(N-n)/N\,. \tag{6}$$

* In the present calculations, an absorption coefficient of $1\cdot0\ \mathrm{cm}^{-1}$ is taken to be typical for a ruby containing $0\cdot05\%$ Cr^{3+}.

In these calculations, the transfer efficiency η_t is computed from two such binomial distributions, namely, the energy absorbed in the laser crystal E_c and the wasted absorption E_w, where

$$E_w = E_P - E_c\,. \tag{7}$$

From equations (3) and (7),

$$\eta_t = E_c/(E_c+E_w)\,. \tag{8}$$

Using the method described by Deming (1943), it can be shown that for two functions F_1 and F_2, of means μ_1 and μ_2 and variances σ_1^2 and σ_2^2, the function $F_1/(F_1+F_2)$ can be approximated, for the case $\sigma_i \ll \mu_i$, by a distribution of mean $\mu_1/(\mu_1+\mu_2)$ and variance σ_3^2 given by

$$\sigma_3^2 = \frac{\mu_1^2\mu_2^2}{(\mu_1+\mu_2)^4}\left[\frac{\sigma_1^2}{\mu_1^2}+\frac{\sigma_2^2}{\mu_2^2}\right]. \tag{9}$$

Using the results of the output summary in place of the means μ_1 and μ_2, values of σ_1^2 and σ_2^2 may be calculated from (6) for $n = E_c$ or E_w and for N the number of tracks. It is thus possible by substituting these in (9) to estimate the variance of η_t for any particular Monte Carlo.

TABLE 1

VARIANCE BETWEEN MONTE CARLOS

Function	Mean* μ	Variance σ^2		Variance Ratio †	σ/μ (%)	
		Theory	Computed		Computed	Theory
E_c	370·7	233·2	160·3	1·45	3·4	4·1
E_w	41·8	40·7	48·7	0·84	16·7	15·3
η_t (%)	89·9	2·07	2·93	0·70	1·9	1·6

* Mean of 10 values.

† Variance ratio for 0·05 significance level is 2·7.

For the case of a perfectly reflecting elliptical cavity of eccentricity 0·4, semi-major axis 12·5 times the source radius, and with ruby and source of equal diameters, the expected variance is shown (as σ^2 theory) in Table 1. The computed variance in Table 1 is derived from a series of 10 Monte Carlos on the same geometry using

$$\sigma^2 = \frac{\Sigma\,(F-\mu)^2}{m-1}, \tag{10}$$

where μ is the mean value of a function F (that is, E_w, E_c, or η_t) and m is the number of Monte Carlos.

Application of the statistical F-test (assuming E_P, E_c, and η_t are approximately normally distributed) shows that the computed variance is not significantly lower than the theoretical at the 0·05 level, and there is thus no evidence that the variance-reduction techniques used have been successful. The inference from Table 1 is thus that for this configuration the efficiency would be quoted as $(89{\cdot}9\pm2{\cdot}8)$%.*

* The 95% probable error is 1·96 times σ (theoretical).

On the other hand, when variances of the energy density are compared (Table 2) for rectangular segments at the ends (outer group) and centre (inner group) of the laser crystal, taken over two runs, it is seen that the variance-reduction techniques have been successful.

V. Computer

The calculation is programmed in the 3600 FORTRAN language for use on a C.D.C. 3600 computer, but is almost completely compatible with I.B.M. FORTRAN IV and, except for the contour-plotting program, is capable of very simple conversion to I.B.M. FORTRAN II. Full details of the program will be found in Defence Standards Laboratories Technical Report No. 277.*

Table 2

VARIANCE WITHIN A MONTE CARLO

Sample	Mean* μ	Variance σ^2		Variance Ratio†	σ/μ (%)	
		Theory	Computed		Computed	Theory
Inner group	45·7	43·7	8·1	5·4	6·2	14·5
Outer group	47·4	45·2	11·4	4·0	7·1	14·2

* Mean of 8 values.

† Variance ratio for 0·05 significance level is 3·2.

A typical series of calculations requires 5 min compilation time and about 3 min for each 1000 track, 20 intersection run, including contour plotting. The number of cards in the data input deck is approximately $10+6M$, where M is the number of components within the cavity.

VI. Results and Discussion

(a) *Comparison with Other Theoretical Treatments*

(i) *Transfer Efficiency*.—Of the theoretical treatments of transfer efficiency reviewed in the Introduction, two (Schuldt and Aagard 1963; Bowness 1965) are in good agreement with each other for the case of a single elliptical cylinder, the simplifications adopted being very similar. The values of the transfer efficiency η_t calculated by Schuldt and Aagard refer to the first reflection from a perfectly reflecting elliptical cylinder into a fully absorbing laser crystal. These show (Fig. 4) that, for a range of eccentricities and for two values of the ratio of laser-crystal radius R_2 to source radius R_1, a sharp fall in efficiency would be expected as the cavity became more elliptical.

Efficiencies estimated by the Monte Carlo technique for the first 20 intersections in a perfectly reflecting cavity, also given in Figure 4, are higher overall and show much less dependence on eccentricity. The adverse effect of a low R_2/R_1 ratio is,

* This report will shortly be available by application to the Chief Superintendent, Defence Standards Laboratories.

however, confirmed. Higher overall efficiencies are an expected outcome of the consideration of multiple reflections in the present work. The modification of Lambert-law emission by refraction at the lamp envelope is a further step towards a realistic simulation of a practical laser configuration and probably accounts both for a proportion of the increased efficiency and for the relative insensitivity to eccentricity foreshadowed by Aagard, Dufault, and Schuldt (1963).

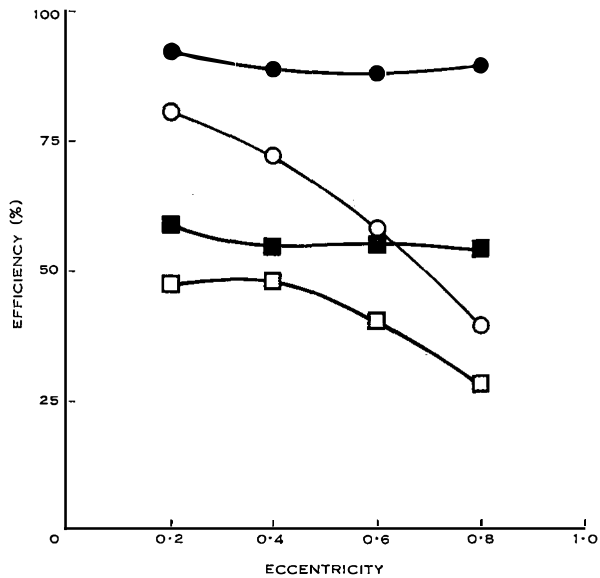

Fig. 4.—Effect of eccentricity on transfer efficiency η_t. ○ $R_2/R_1 = 1\cdot0$, Schuldt and Aagard (1963); ● $R_2/R_1 = 1\cdot0$, Monte Carlo; □ $R_2/R_1 = 0\cdot5$, Schuldt and Aagard; ■ $R_2/R_1 = 0\cdot5$, Monte Carlo. $R_1/a = 0\cdot08$ in all cases. R_1 = radius of flash-lamp, R_2 = radius of laser crystal, and a = semimajor axis of ellipse.

(ii) *Energy Density Distribution.*—A computation was made on a system comprising a circular diffusing cylinder with an axial ruby rod, four symmetrically disposed flash tubes, and different ruby to lamp spacings, D (see Fig. 1). For the following data: ruby 6 by $\frac{3}{8}$ in., absorption coefficient $1\cdot0\ \mathrm{cm}^{-1}$; reflectance 99% diffuse, 1% absorption; lamps E.G.&G. FX 45, internal diam. 7 mm, outside diam. 9 mm, length 6 in.; distance from flash-lamp surface to cavity wall $0\cdot354$ in. ($2R_1$), the efficiencies were computed for values of D/R_1 as:

D/R_1	4	8	16
η_t (%)	51·8	37·5	25·4

The energy density distributions are given in Figure 5. The case $D/R_1 = 16$ probably

Fig. 5 (*opposite page*).—Contour diagrams for systems with cylindrical diffusing cavities.
(*a*) $D/R_1 = 4$, end segment; (*b*) $D/R_1 = 4$, centre segment;
(*c*) $D/R_1 = 8$, end segment; (*d*) $D/R_1 = 8$, centre segment;
(*e*) $D/R_1 = 16$, end segment; (*f*) $D/R_1 = 16$, centre segment.
D = separation (see Fig. 1) and R_1 = lamp radius. The outline of the laser crystal is shown.

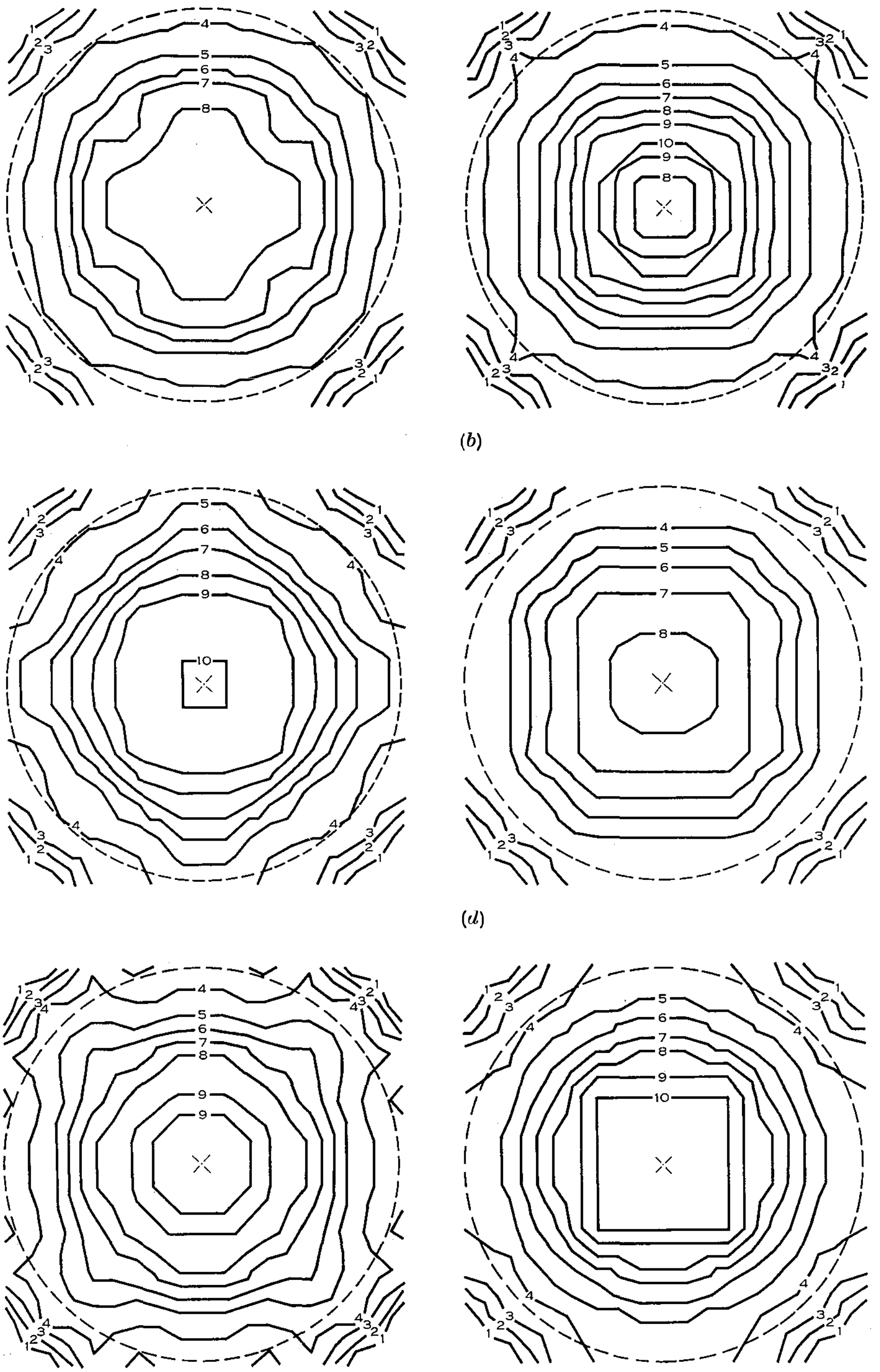

(a) (b) (c) (d) (e) (f)

gives a reasonable approximation to isotropic illumination of the ruby crystal as investigated analytically by Sooy and Stitch (1963), ignoring the effect of internal reflections within the crystal; they produced curves of normalized energy density E/E_{max} as a function of normalized radius R/R_1 relating to a number of normalized absorption coefficients aR_2, where a is the absorptivity and R_2 is the radius of the ruby rod.

In Figure 6, points derived from the contours of energy density distribution (Fig. 5 (*f*)) for $D/R_1 = 16$, having $aR_2 = 0\cdot 96$, are compared with the curve of Sooy and Stitch for $aR_2 = 1\cdot 00$. Thus, in this simple case where an analytical solution is possible, the agreement is excellent and confirms the reliance that may be placed on the other contour plots.

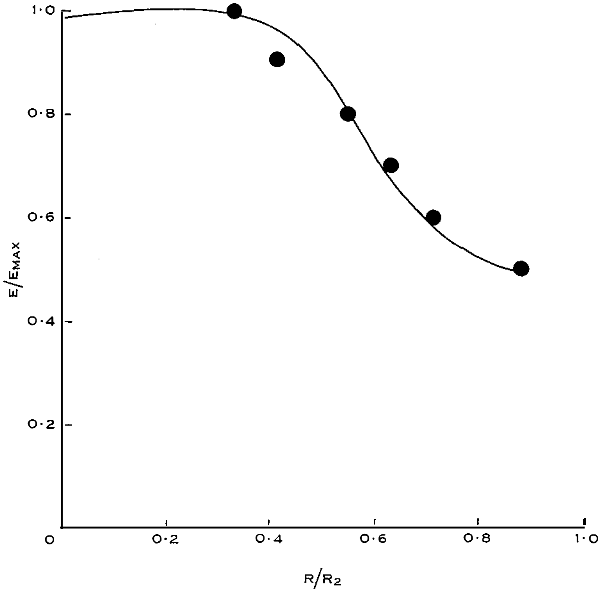

Fig. 6.—Variation of energy density along a radius of the laser crystal; E/E_{max} = normalized energy, R/R_2 = normalized radius; — curve of Sooy and Stitch (1963); ● points from contours of Figure 5(*f*).

(*b*) *Comparison with Experiments on Ruby Lasers*

(i) *Single-lobe and Four-lobe Geometry*.—Since no actual measurements of transfer efficiency have been reported, comparisons with experiment must be made indirectly through threshold levels and total efficiency η_T.

A comparison between single-lobe and four-lobe ellipses has been reported in some detail by Bowness, Missio, and Rogala (1962, 1963). The inclusion of dimensional data enabled a parallel Monte Carlo simulation to be made. The results are summarized in Table 3. There is an apparent disagreement between the calculated and experimental results in that the product $\eta_L . \eta_c$ is not constant. Since similar lamps are used in both configurations, η_L is expected to be constant. However, analysing the components of η_c we have

$$\eta_c = \Phi \eta \eta_l F(t_1, t_2, \epsilon) , \tag{11}$$

where Φ is the quantum conversion factor $\lambda_{in}/\lambda_{out}$, η is the fluorescent quantum efficiency, $F(t_1, t_2, \epsilon)$ is a function of resonator mirror transmittances and intrinsic resonator loss including scattering and diffraction losses, and η_l is the lasing efficiency of the crystal. For this purpose, the lasing efficiency η_l is defined as the ratio of stimulated output energy to total emission from the whole crystal at the laser wavelength. Of the factors comprising η_c, only Φ and η are functions of the laser crystal; ϵ, t_1, and t_2 are functions of the resonating cavity as a whole and η_l is a property of the pumping system. It is clear that, in the configurations considered in Table 3, the only factor that may vary between the two pump-cavity designs is η_l. Since lasing may be achieved without necessarily pumping all parts of the crystal above threshold (G. Mayer, cited after Sooy and Stitch 1963; Congleton *et al.* 1964), η_l is clearly a function of energy density distribution within the crystal and of pumping level.

TABLE 3

COMPARISON OF SINGLE- AND FOUR-LOBE CAVITIES*

No. of Lobes	Computed η_t (%)	Experimental Output† (J/lobe)	Experimental η_T (%)	$\eta_L \cdot \eta_c$‡ (%)
1	36·2	15	0·75	2·1
4	17·4	17·5	0·62	3·5

* Data used: ruby 6 by $\frac{3}{8}$ in., absorption coefficient $1\cdot0$ cm^{-1}; ellipse semimajor axis 4 in., semiminor axis 2·5 in., length 6 in.; reflectance 86% specular, 2% diffuse, 12% absorption; lamps E.G. & G. FX 45, internal diam. 7 mm, outside diam. 9 mm, length 6 in.

† For 2KJ flash lamps.

‡ $\eta_L \cdot \eta_c = \eta_T$(experimental)/$\eta_t$(computed).

The contour diagrams (Fig. 7) show that the energy distribution is much more even for the four-lobe configuration than in the single-lobe case, and it is therefore reasonable that η_l should be different for the two systems; this would explain the observed variation in η_c. It is interesting that, in the four-lobe case, there is an annular distribution of energy density within the ruby, a possibility shown experimentally by Skinner (1964). A further irregularity in energy density distribution is shown in Figure 7(*a*), where, although the lamp is situated (as always) to the right of the ruby, the peak of energy density is offset to the left, demonstrating that, in this elliptical configuration, the contribution due to that portion of the ellipse close to the ruby is much greater than that due to direct coupling of the lamp to the ruby. The effect of direct coupling is shown, however, in Figure 5, in which there is a tendency for peaks of energy density to appear adjacent to the four lamps as these are moved closer to the ruby. The effects of direct coupling in an elliptical cavity have been demonstrated by Daneu, Sacchi, and Svelto (1964), who observed an offset in peak intensity towards the lamp when the laser crystal was relatively close to the lamp.

(ii) *Effect of Reflector Properties*.—The effect of using different reflector materials in a typical single-lobe elliptical cylinder is shown in Table 4, which well demonstrates the strong dependence of efficiency η_t on reflector properties. On the assumption,

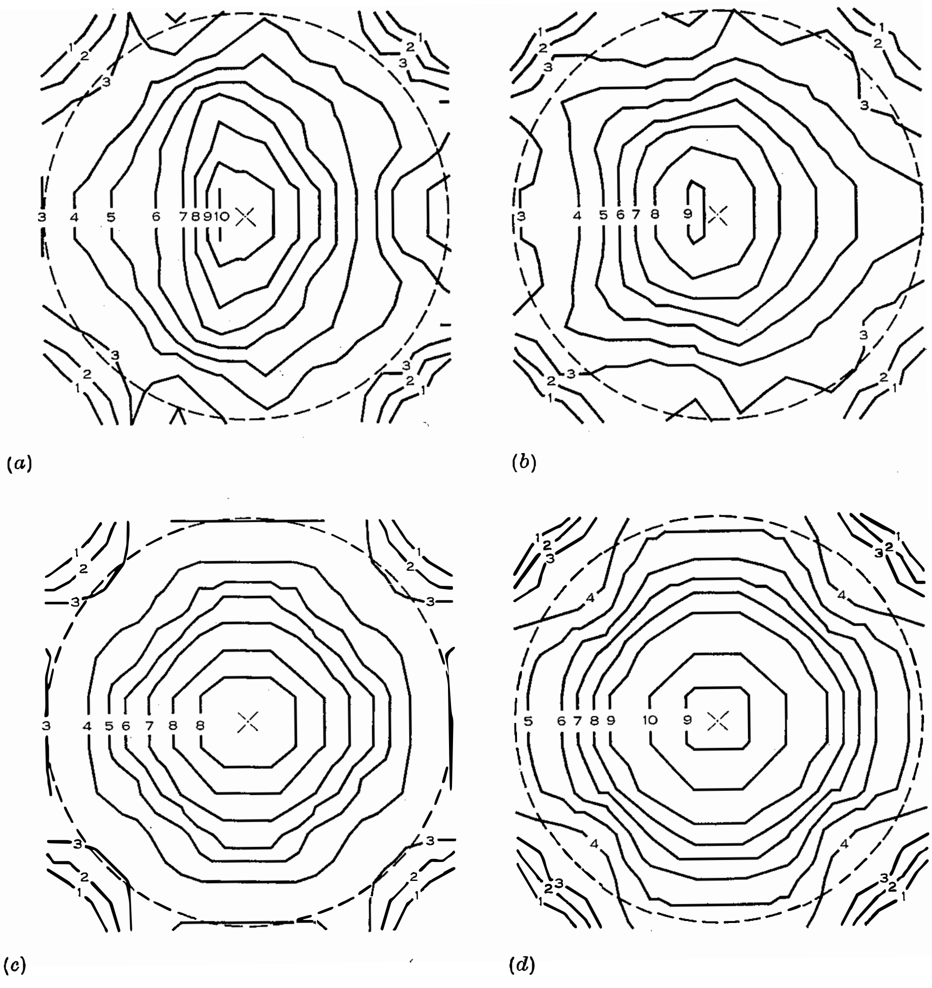

Fig. 7.—Contour diagrams for single- and four-lobe elliptical cylinders.

(*a*) Single lobe, end segment; (*b*) single lobe, centre segment;
(*c*) four lobe, end segment; (*d*) four lobe, centre segment.

supported by detailed examination of Monte Carlo histories, that a ray loses most of its energy in the first pass through the ruby, the slope of the log η_t versus log(total reflectivity) plot approximates to the average number of reflections at the cavity wall. The data for specular reflectors given in Table 4 lie on a line of slope $7 \cdot 3$ when so treated, while the existence of a diffuse component in low total reflectivities results in efficiencies greatly above the extrapolated line. An actual count of intersections at the cavity gives a value of 7·5 for all three specular reflectors. This supports the assertion in Section VI(*a*) that the allowance for multiple reflection is mainly responsible for the higher efficiencies forecast by the Monte Carlo technique as compared with those of Schuldt and Aagard.

Congleton *et al.* (1964), reporting on an unspecified elliptical geometry, state that an increase in reflectance from 84 to 92% halves the threshold. An assumption that the efficiency is thereby doubled, implying that η_l is constant, leads to an estimate of 7·6 as the average number of reflections. This is in excellent agreement with the values of 7·3 and 7·5 deduced from the Monte Carlo calculations as described above.

TABLE 4

EFFECT OF CAVITY REFLECTANCE ON EFFICIENCY*

Cavity Material	Specular Reflectance (%)	Diffuse Reflectance (%)	Absorption (%)	η_t† (%)
—	100	0	0	88·9
—	98	0	2	75·5
—	95	0	5	61·4
Polished Al	86‡	2‡	12	40·8
Anodized Al	68‡	10‡	22	23·4

* Data used: ruby 3 by ¼ in., absorption coefficient 1·0 cm^{-1}; ellipse semimajor axis 1·25 in., semiminor axis 1·146 in., length 3 in.; lamps E.G. & G. FX 42, internal diam. 7 mm, outside diam. 9 mm, length 3 in.

† Extrapolated to an infinite number of intersections.

‡ Typical experimental results.

VII. Summary and Conclusions

A method has been developed for the simultaneous evaluation of the transfer efficiency and energy density distribution in the crystal for a wide variety of laser pumping configurations, by means of tracing the paths of light rays both inside and outside the crystal. In this way the effects of multiple reflections and of different crystal absorptivities may be studied. In addition, the method greatly extends the scope of present techniques for evaluating pumping systems in that account may be taken of the effects, not only of specular and diffuse reflections at the cavity wall, but also of water jackets around flash-lamps and of a variety of schemes for utilizing fluorescent materials to increase pumping efficiency. Allowance is made for the modification of Lambert-law emission due to refraction at the flash-lamp envelope; this is made possible by the three-dimensional approach adopted.

Where results can be compared with previous analyses of idealized systems and with experimental work, the agreement is generally good. The role of refraction at the lamp envelope in reducing the expected sensitivity of elliptical cavities to eccentricity has been established; however, such systems have also been shown to be very sensitive to the reflective properties of the cavity walls. The importance of uniform energy density distribution within the laser crystal for the achievement of high overall efficiencies has been demonstrated. The method can clearly be used with advantage for optimizing the design of laser pumping cavities.

VIII. Acknowledgments

The authors wish to thank Mr. R. Maine of the Bureau of Meteorology, Melbourne, for useful information on the technique of contour printing. This paper is published by permission of the Chief Scientist, Australian Defence Scientific Service, Department of Supply, Melbourne.

IX. References

Aagard, R. L., Dufault, R. A., and Schuldt, S. B. (1963).—*Appl. Opt.* **2**: 540.
Ackerman, J. A. (1963).—*Proc. Inst. Electl Electron. Engrs* **51**: 1032–3.
Bowness, C. (1965).—*Appl. Opt.* **4**: 103–7.
Bowness, C., Missio, D., and Rogala, T. (1962).—*Proc. Inst. Radio Engrs* **50**: 1704–5.
Bowness, C., Missio, D., and Rogala, T. (1963).—*Proc. Inst. Electl Electron. Engrs* **51**: 254–5.
Ciftan, M., Luck, C. F., Shafer, C. G., and Statz, H. (1961).—*Proc. Inst. Radio Engrs* **49**: 960–1.
Congleton, R. S., Sooy, W. R., Dewhirst, D. R., and Riley, L. D. (1964).—"Quantum Electronics—Paris 1963 Conference." pp. 1415–25. (Columbia Univ. Press: New York.)
Cooke, C. H., McKenna, J., and Skinner, J. G. (1964).—*Appl. Opt.* **3**: 957–61.
Daneu, V., Sacchi, C. A., and Svelto, O. (1964).—*Alta Freq.* **33**: 198E–199E.
Deming, W. E. (1943).—"Statistical Adjustment of Data." pp. 38–41. (Wiley: New York.)
Devlin, G. E., McKenna, J., May, A. D., and Schawlow, A. L. (1962).—*Appl. Opt.* **1**: 11–15.
Emmett, J. L., Schawlow, A. L., and Weinberg, E. H. (1964).—*J. Appl. Phys.* **35**: 2601–4.
Fried, D. L., and Eltgroth, P. (1962).—*Proc. Inst. Radio Engrs* **50**: 2489.
Householder, A. S. (1949).—*Appl. Math. Ser.* **12**: Foreword.
Li, T., and Sims, S. D. (1962).—*Proc. Inst. Radio Engrs* **50**: 464–5.
McKenna, J. (1963).—*Appl. Opt.* **2**: 303–10.
Rotenberg, A. (1960).—*J. Ass. Comput. Mach.* **7**: 75–7.
Schuldt, S. B., and Aagard, R. L. (1963).—*Appl. Opt.* **2**: 509–13.
Skinner, J. G. (1964).—*Appl. Opt.* **3**: 963–5.
Sooy, W. R., and Stitch, M. L. (1963).—*J. Appl. Phys.* **34**: 1719–23.
Tomiyasu, K. (1962).—*Proc. Inst. Radio Engrs* **50**: 2488–9.

Appendix

Use of Random Numbers in Determination of Ray Paths

(*a*) *General*.—When a ray reaches a point at which its path divides, a random choice is made between the available routes in such a way that, if an indefinitely large number of rays were considered, the cumulative probability distribution of energy in the rays with respect to a variable x would obey the appropriate physical law. It is required to simulate such a system by using a pseudo-random number generator to produce an effectively random series of numbers R, evenly distributed between 0 and 1, corresponding to the distribution of the energy in the rays with respect to x. This is achieved by making R equal to the cumulative probability function in terms of x, since this function is also evenly distributed between 0, when x is at its minimum, and 1, when x is at its maximum. The cumulative probability function can be derived from the probability density function by integration in the case where the latter function is defined by the physical law.

(*b*) *Lambert-law Emission.*—Lambert's law states that the energy flux in a small solid angle $\delta\omega$ about a line inclined at an angle θ to the surface normal is proportional to $\cos\theta\,.\,\delta\omega$ and is independent of ϕ, the azimuth angle. This law is taken to apply to emission from a plasma surface or an opaque fluorescent surface, and to diffuse reflection.

Since θ and ϕ are independent, they may be considered separately. The solid angle inclined between θ and $\theta+\delta\theta$ is

$$\delta\omega = 2\pi\sin\theta\,.\,\delta\theta\,, \tag{A.1}$$

so the total energy flux between θ and $\theta+\delta\theta$ is proportional to $\cos\theta\,.\,\delta\omega$, that is, to $\sin 2\theta\,.\,\delta\theta$. Thus the the probability density function is

$$\begin{aligned} f(\theta) &= \sin 2\theta\left\{\int_0^{\frac{1}{2}\pi} \sin 2\theta\,.\,\mathrm{d}\theta\right\}^{-1} \\ &= \sin 2\theta\,. \end{aligned}$$

From Section (*a*) it is thus possible to set θ by a random number R according to the equation

$$\begin{aligned} R &= \int_0^{\theta} \sin 2\theta\,.\,\mathrm{d}\theta \\ &= \tfrac{1}{2}(1-\cos 2\theta)\,, \end{aligned}$$

so that

$$\theta = \tfrac{1}{2}\cos^{-1}(1-2R)\,. \tag{A.2}$$

Since ϕ is evenly distributed between 0 and 2π, the same approach leads to the equation

$$\phi = 2\pi R'\,, \tag{A.3}$$

R' being a second random number.

(*c*) *Isotropic Emission.*—The flux in isotropic emission is independent of both inclination θ and azimuth ϕ, that is, the flux in a solid angle $\delta\omega$ is $\delta\omega/4\pi$. This is assumed to apply to fluorescent emission within a phosphor solution. An integration similar to that above leads to the equations

$$\theta = \cos^{-1}(1-2R)\,, \tag{A.4}$$

$$\phi = 2\pi R'\,. \tag{A.5}$$

(*d*) *Penetration Depth.*—The intensity of a light beam in an absorbing medium varies as $\exp(-ax)$, where a is the absorptivity of the medium and x the distance along the ray. This is considered to apply to absorption by a laser crystal or a phosphor solution.

The probability density function $f(x)$ for a penetration depth x must be proportional to $\exp(-ax)$; the probable penetration depth can be shown to be

$$x = (1/a)\ln(1-R)\,. \tag{A.6}$$

(*e*) *Choice of Refraction or Reflection.*—When a light ray strikes a refracting surface, the proportion P of reflected intensity is, from the Fresnel equations,

$$P = \tfrac{1}{2}\frac{\sin^2(i-r)}{\sin^2(i+r)} + \tfrac{1}{2}\frac{\tan^2(i-r)}{\tan^2(i-r)}, \tag{A.7}$$

where i is the angle of incidence and r the angle of refraction. This applies to the surfaces of laser crystals, lamp envelopes, water jackets, and sapphire cladding for rubies.

Since only two discrete paths are available, the principles of Section (*a*) above cannot be applied; the probability P is compared with the random number R and a reflected path is computed if $R \leqslant P$; if $R > P$, a refracted path is computed. If a large number of rays are considered, the correct fraction will thus be reflected.